CHAPTER IV
RESULTS AND DISCUSSION

4.1 TOF as a Function of NO Concentrations and Temperatures

From the thermogravimetric analyzer (TGA) results, the rate of weight change in graphite during NO gasification reaction was measured with time. The NO gasification rates were calculated from the rate of graphite reacted and the rate of CO_2 formation, by using the following stoichiometric reactions:

$$C + NO \longrightarrow CO + \tfrac{1}{2} N_2$$

$$C + 2NO \longrightarrow CO_2 + N_2$$

A typical TGA result is shown in Figure 4.1. The result shows that the reaction rate slightly increases with time at very low burnoff levels and then becomes constant at about 10% burnoff. However, the reaction rate changes again at very high burnoff levels. Therfore only reaction rates between 10% and 20% burnoff were used in this work.

Because graphite samples used in this study were graphitic carbon with well-defined structure then the edge plane surface areas could be calculated from the geometry of the graphite flakes. It is evident that the edge plane surface areas are the active sites of the NO-carbon reaction. Thus TOF or rate based per active site could be calculated by using the active surface areas of the graphite.

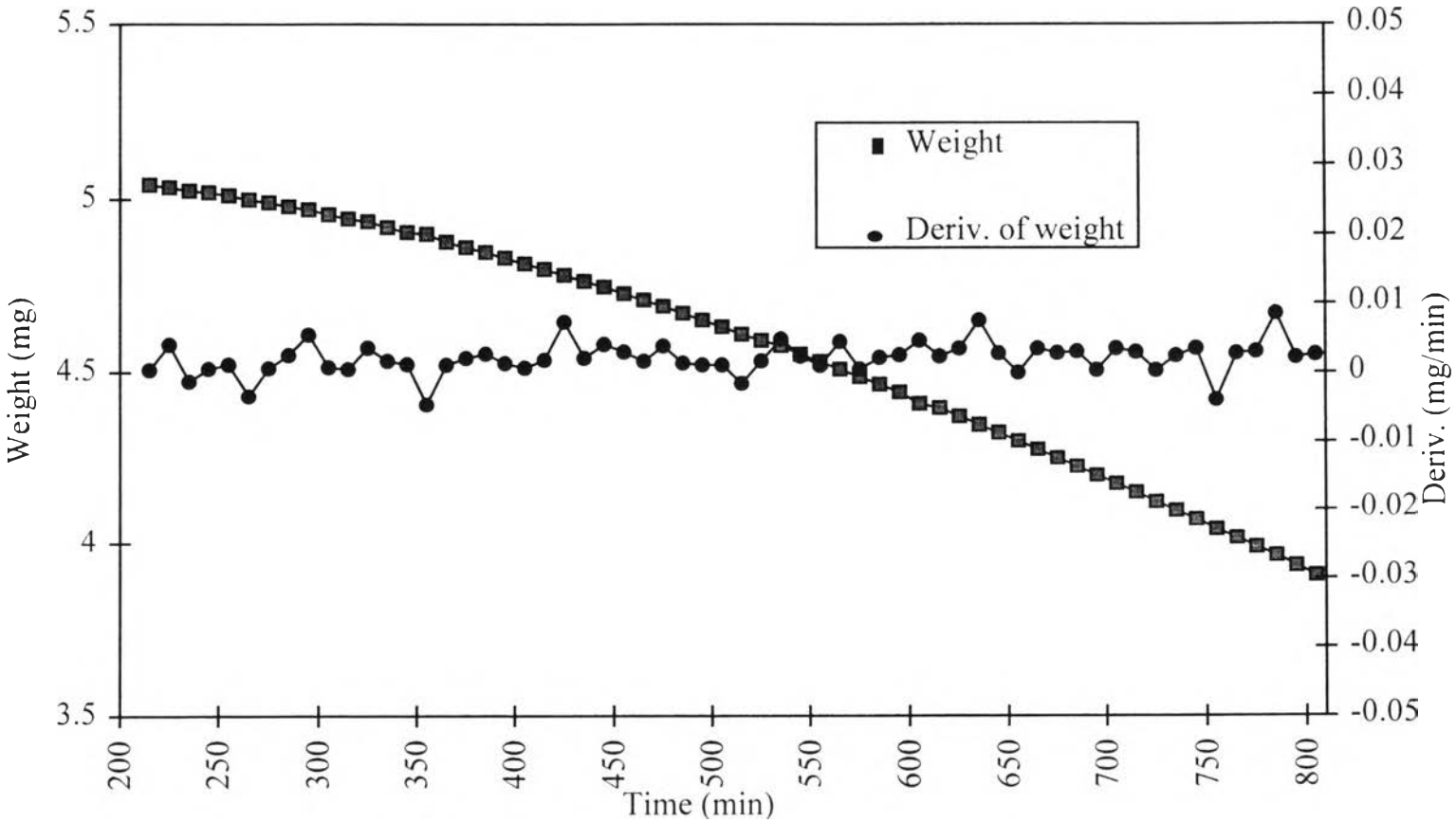

Figure 4.1 TGA result of SP-1 graphite at 6% NO concentration and temperature 550 °C.

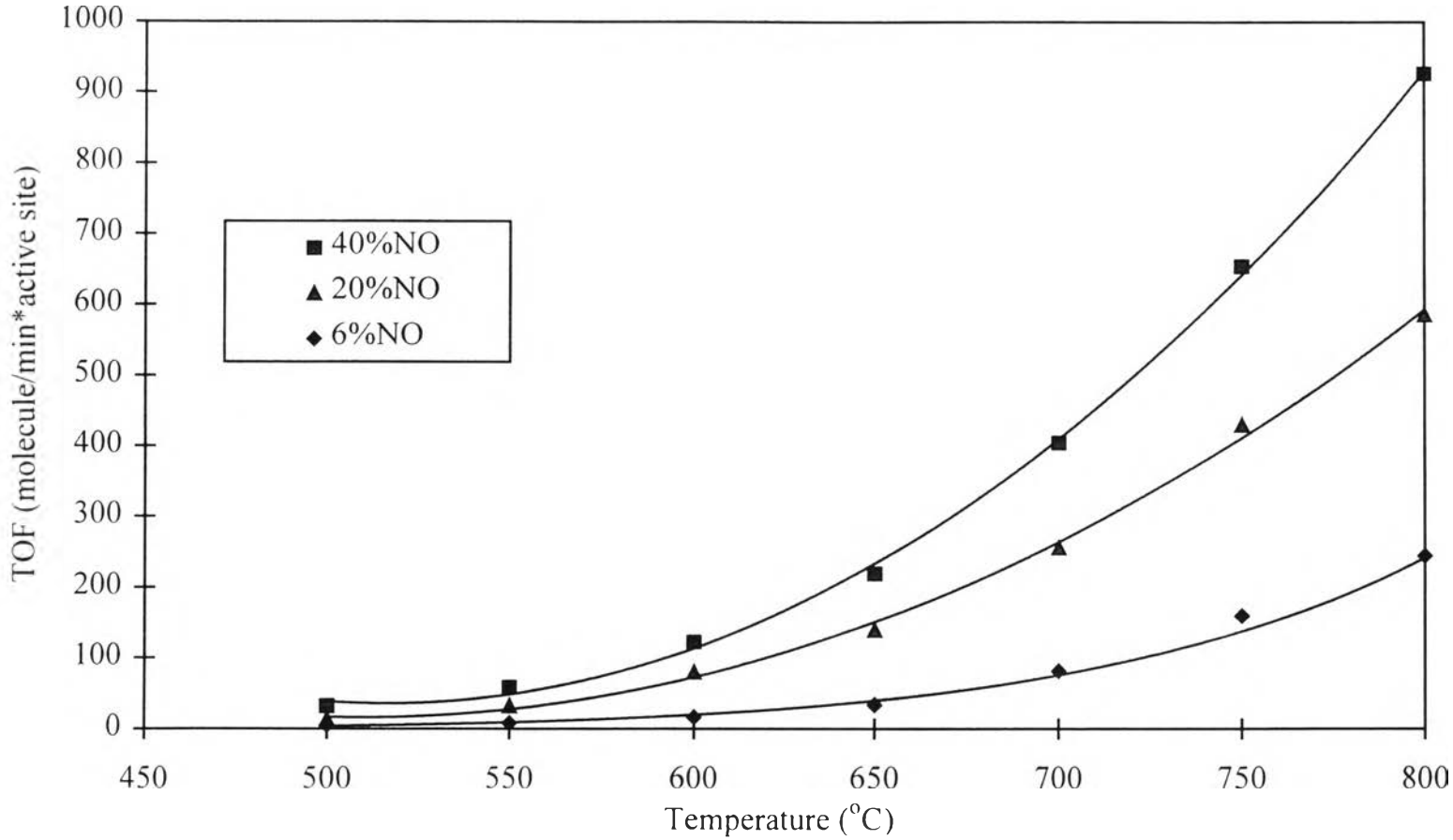

Figure 4.2 TOF of micro 450 graphite vs. temperature.

Figure 4.2 illustrates temperature-dependent changes in the TOF rates of NO gasification reactions for different NO concentrations of micro 450 graphite. As can be seen from this figure, at constant NO concentration, TOF is increased when either gasification temperature or NO concentration increases. This result indicated that the gasification temperature and the NO concentration had effect on the TOF of the NO gasification reaciton.

The dependency of the TOF on the reaction temperature and initial NO concentration can be represented by the following equation:

$$r = A_0 P_{NO}^{a} e^{(-Ea/RT)}$$

where R is the universal gas constant, A_0 is the preexponential factor, a is the kinetic order with respect to NO, Ea is the activation energy and T is the reaction temperature.

Figure 4.3 illustrates temperature-dependent changes in the TOF rates of NO gasification reaction for different NO concentration of SP-1 graphite. It also shows the same tendency as for micro 450. The NO concentration has effect on the NO gasification reaction and the TOF rates are increased with increasing temperature.

Figures 4.4, 4.5 and 4.6 show the relationships between the NO gasification rate and the edge surface area at temperature between 500-800 °C. Rate increases as the edge surface area increases for the entire range of observed temperatures. These results are in good agreement with the work of Chen and Yang (1993). In their work, the similar trend was observed in which the gasification rate of O_2 (expressed in g/g.hr) increased with increasing edge surface area.

Figures 4.7, 4.8 and 4.9 show the effects of temperature on TOF of the NO gasification with micro 450 and SP-1 graphites at 6%, 20% and 40%,

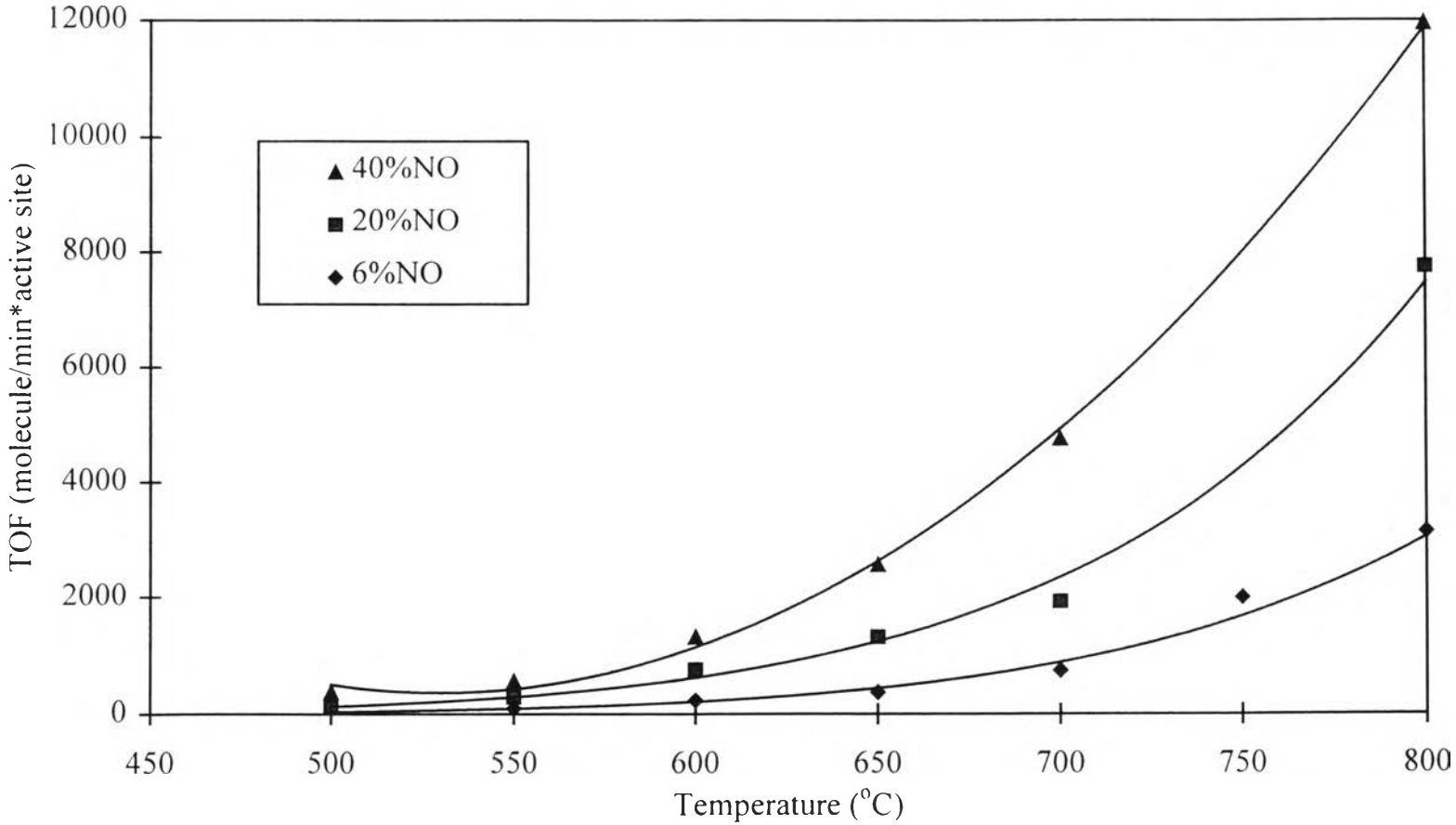

Figure 4.3 TOF of SP-1 graphite vs. temperature.

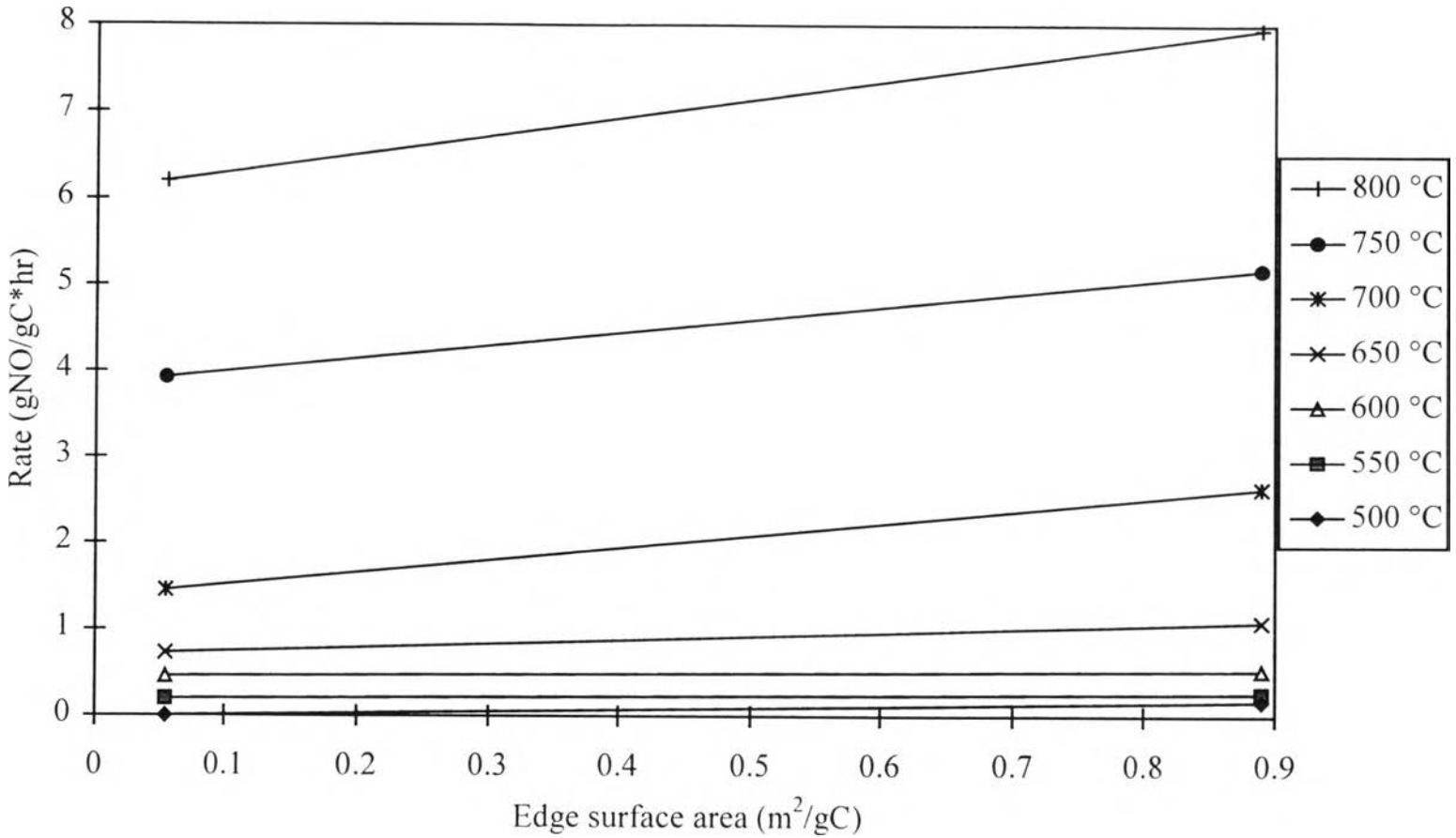

Figure 4.4 Plot of NO reduction rate vs. edge surface area at NO concentration of 6% and various temperatures for different graphites used.

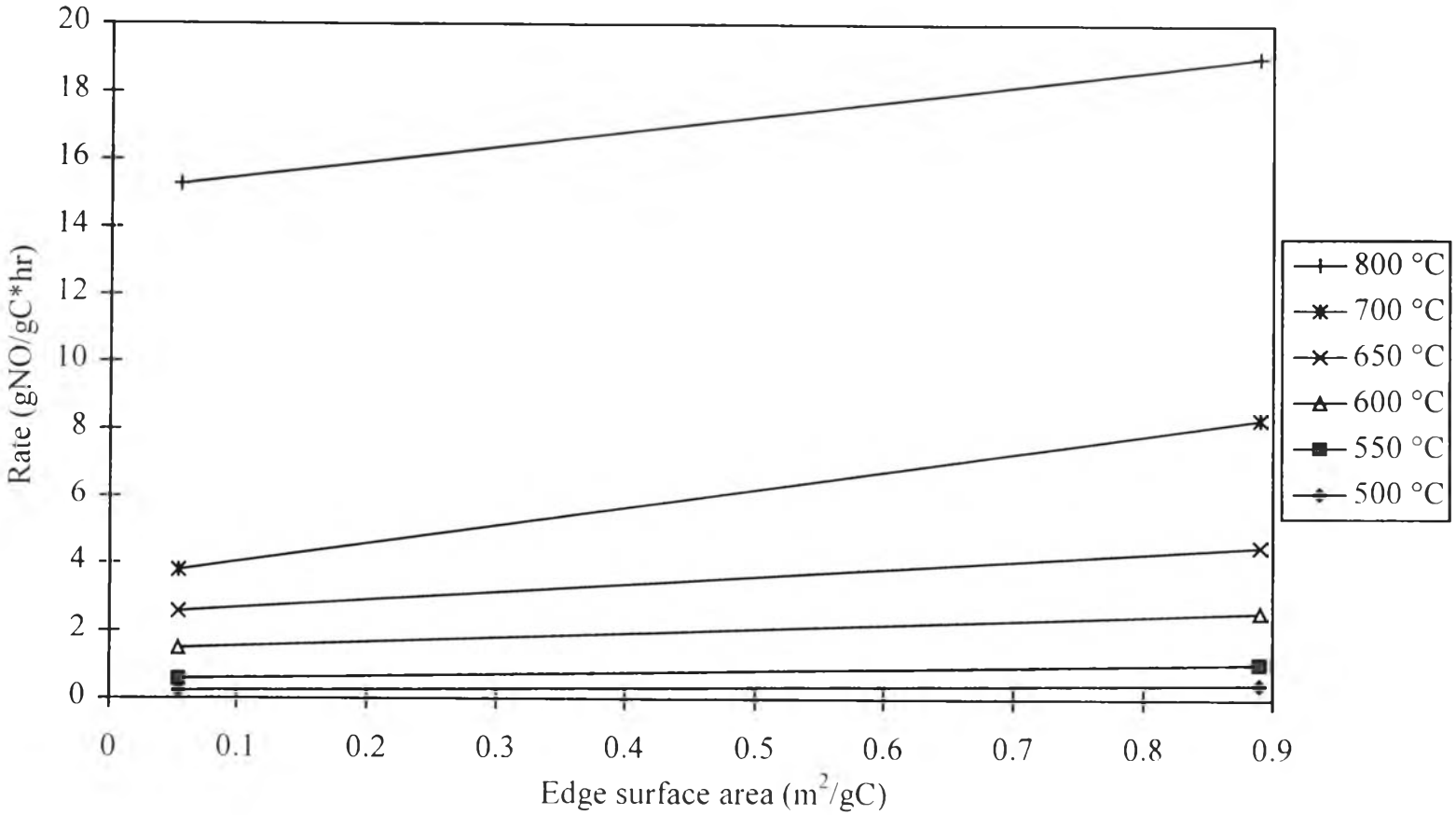

Figure 4.5 Plot of NO reduction rate vs. edge surface area at NO concentration of 20% and various temperatures for different graphites used.

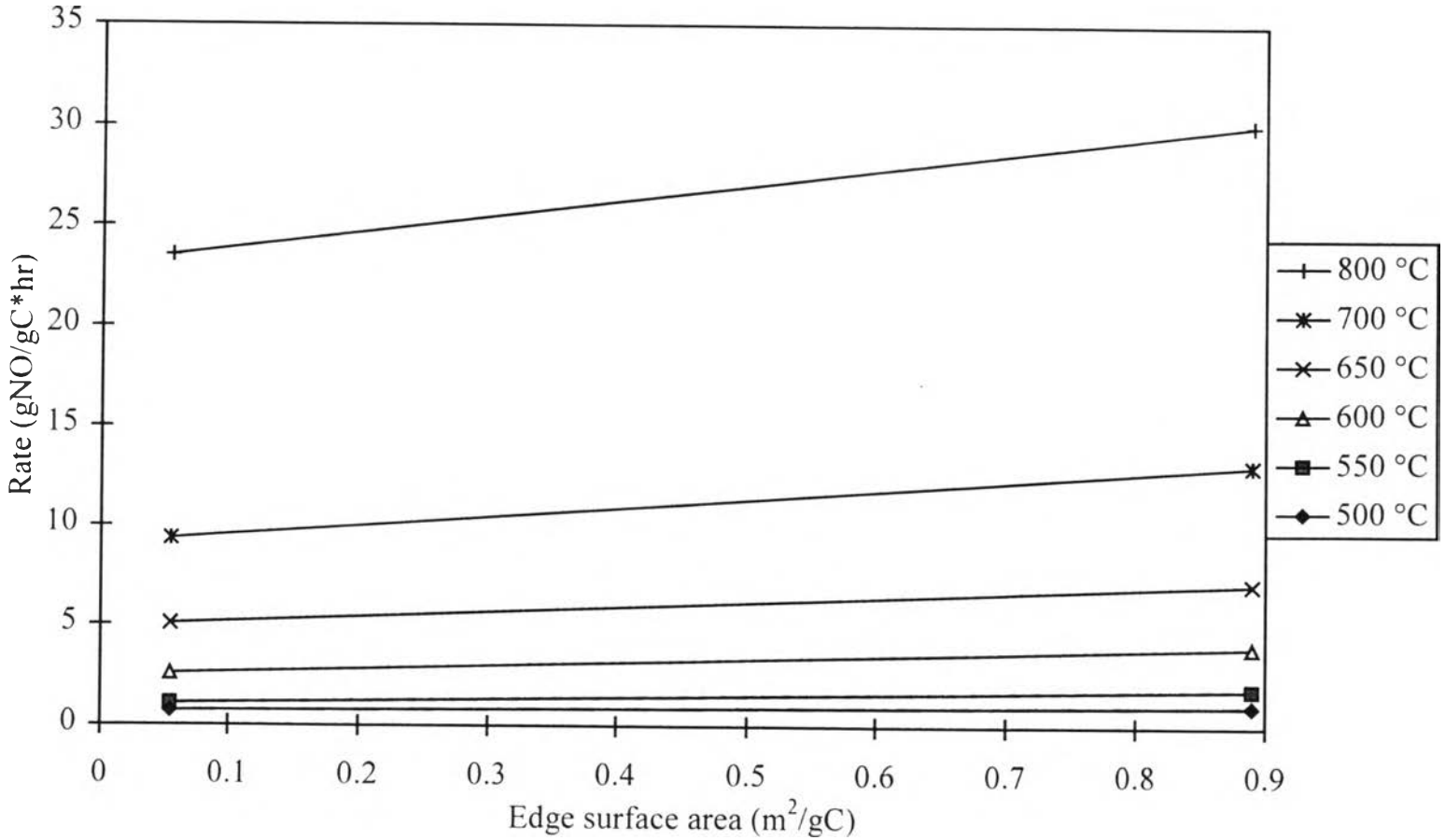

Figure 4.6 Plot of NO reduction rate vs. edge surface area at NO concentration of 40% and various temperatures for different graphites used.

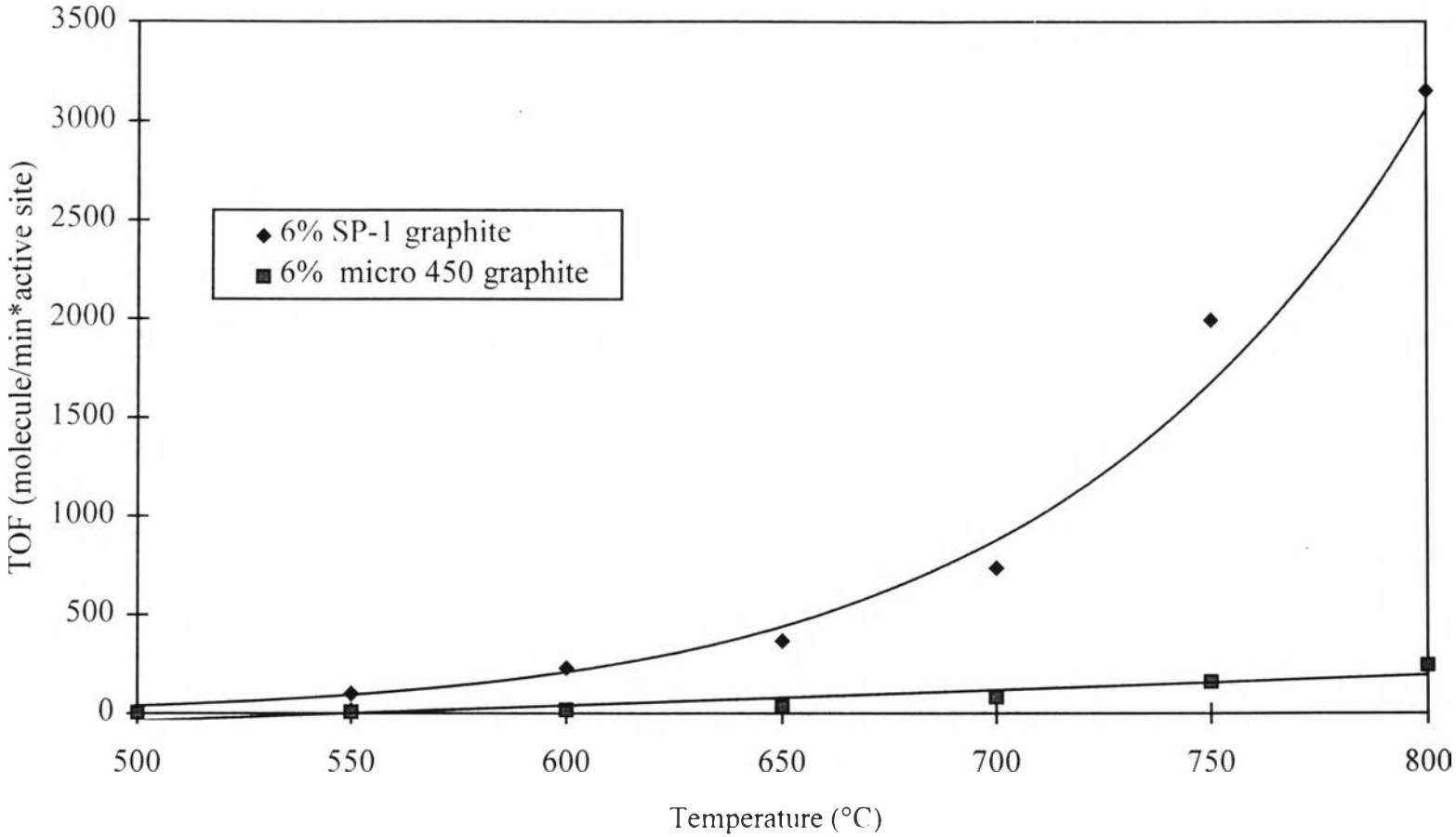

Figure 4.7 TOF as a function of temperature for different graphite samples at 6% NO concentration.

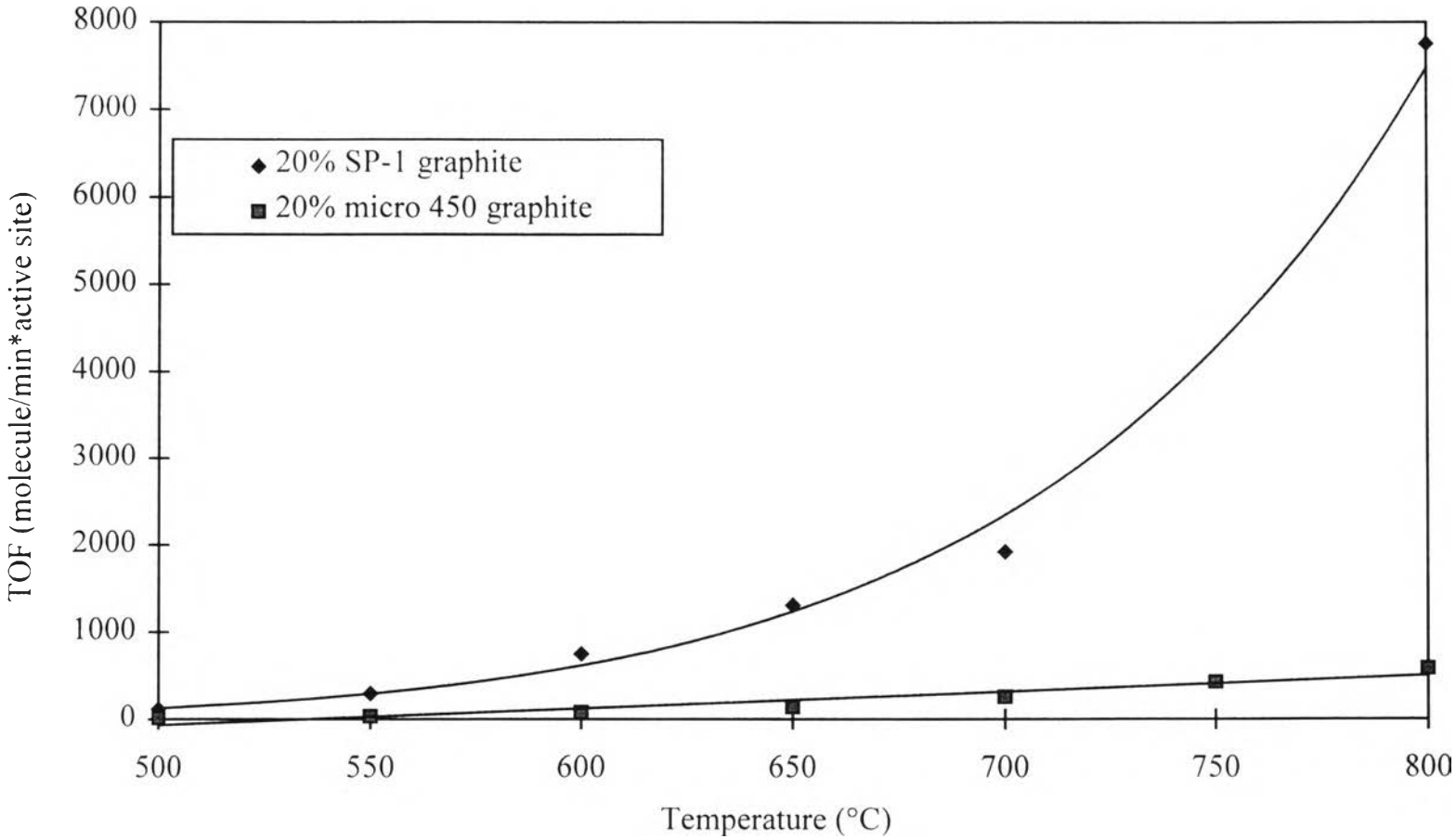

Figure 4.8 TOF as a function of temperature for different graphite samples at 20% NO concentation.

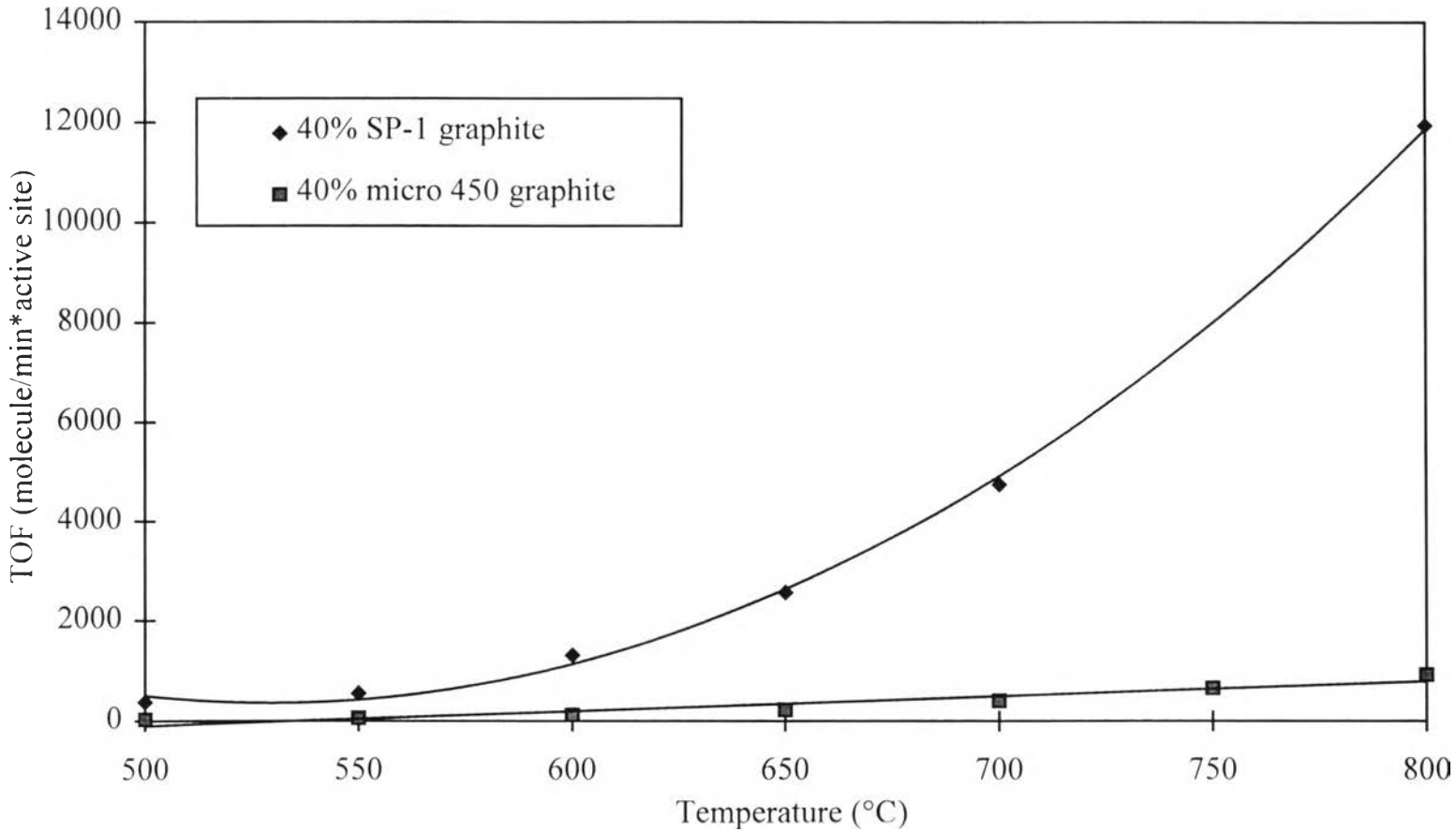

Figure 4.9 TOF as a function of temperature for different graphite samples at 40% NO concentration.

respectively. For all observed concentrations, the TOF of SP-1 was greater than that of micro 450. This is surprising because the micro 450 graphite has higher edge surface area than the SP-1 graphite so that the micro 450 graphite should have higher TOF than the SP-1 graphite. However, from the aforementioned results (Figures 4.4, 4.5 and 4.6) the reaction rates expressed as mass of NO per mass of graphite per unit time were higher for micro 450 than for SP-1 graphite. In fact, if initial surface areas are low, even small increases in area during reaction can be significant (Aarna and Suuberg, 1997). However, the edge surface areas used in this work were determined before running the experiment. It is likely that the edge surface areas might be underestimated if surface areas were increased during reaction.

For SP-1 graphite, its particle size is quite large compared to the micro 450 graphite. If an increase in edge surface area took place during reaction, the edge surface area of SP-1 graphite would be significantly increased. As a result, it is possible that a higher TOF observed for SP-1 graphite may be due to the underestimated edge surface area.

4.2 The Order of Reaction

The typical power rate law for the heterogeneous NO destruction rate expression was defined as

$$r = kP_{NO}^{a}$$

where r = NO molar reaction (destruction) rate per unit solid surface area per time per unit of NO pressure;

P_{NO} = the initial partial pressure of NO;

a = kinetic order of NO;

k = rate constant.

Taking the natural logarithm on both sides of the above equation yields

$$\ln r = \ln k + a \ln P_{NO}$$

Therefore, if a straight line is obtained from the plot of the rate and partial pressure of NO, the kinetic order of NO can be directly determined from its slope.

Figures 4.10 and 4.11 illustrate the kinetics order of the NO gasification reaction with respect to NO for the micro 450 graphite and the SP-1 graphite respectively. It can be seen that straight lines are obtained for both graphites used. In the low temperature regime (below 650 °C), the slopes of the plots are close to unity. This indicates that the reduction of NO by graphite at low temperature is the first order reaction with respect to initial NO pressure which is in agreement with the results of Furusawa et al. (1980).

However, the slopes between 0.70 and 0.90 have been found at temperatures above 650 °C. This may be because of the effect of CO on the reaction rate. In fact CO was observed as a product at higher temperatures. This occurring CO can subsequently react by the possibility of surface catalyzed reaction:

$$CO + NO \longrightarrow CO_2 + \tfrac{1}{2} N_2$$

As a result, CO can behave as both product and reactant gases at the same time. Aarna et al. (1997) found that even low levels of CO can significantly affect the observed reaction order. Thus the reaction order with respect to NO was decreased due to the presence of CO in the high temperature regime.

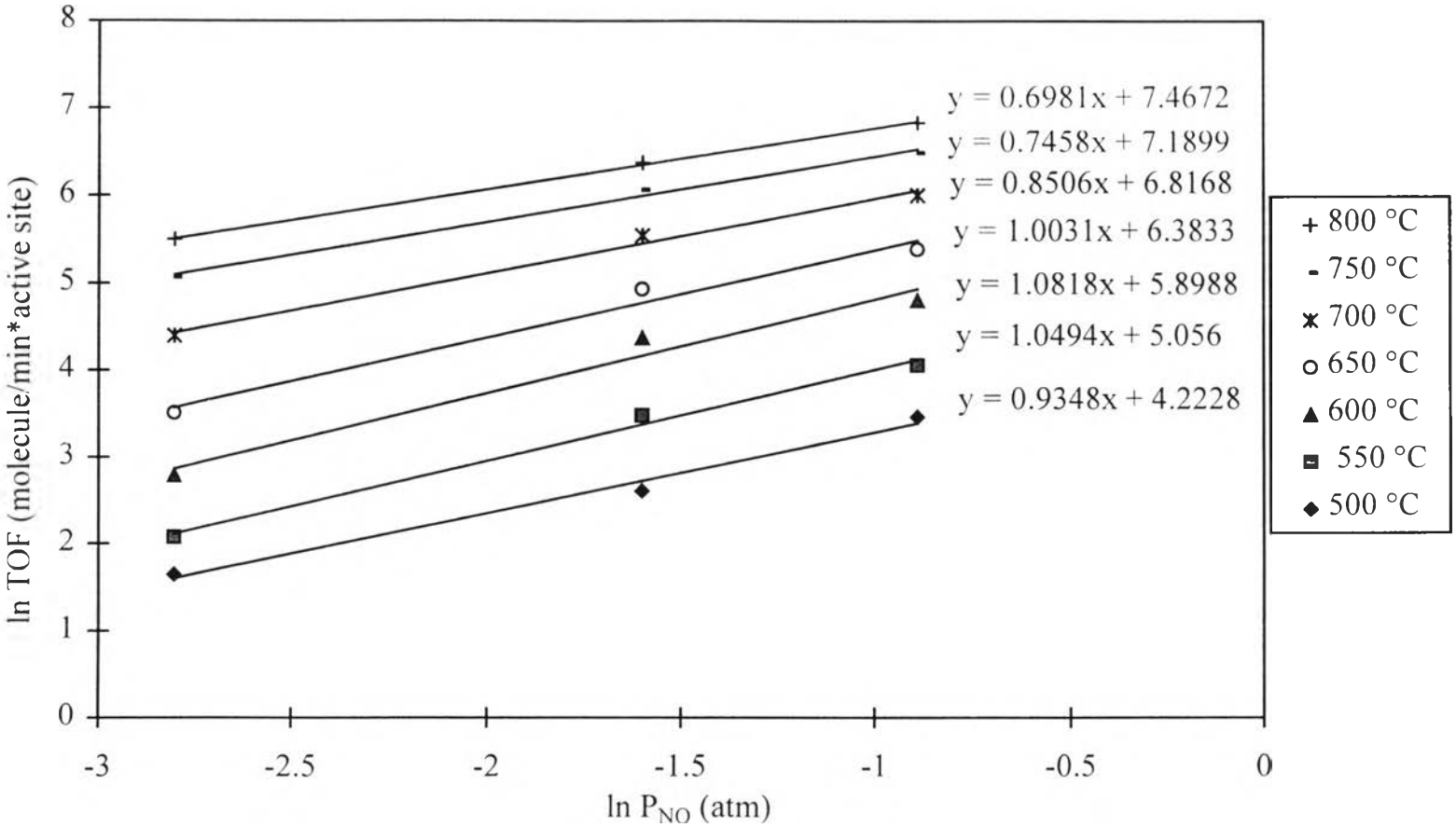

Figure 4.10 Relation between the initial pressure of NO and TOF of NO reduction with micro 450 graphite at temperature between 500-800 °C.

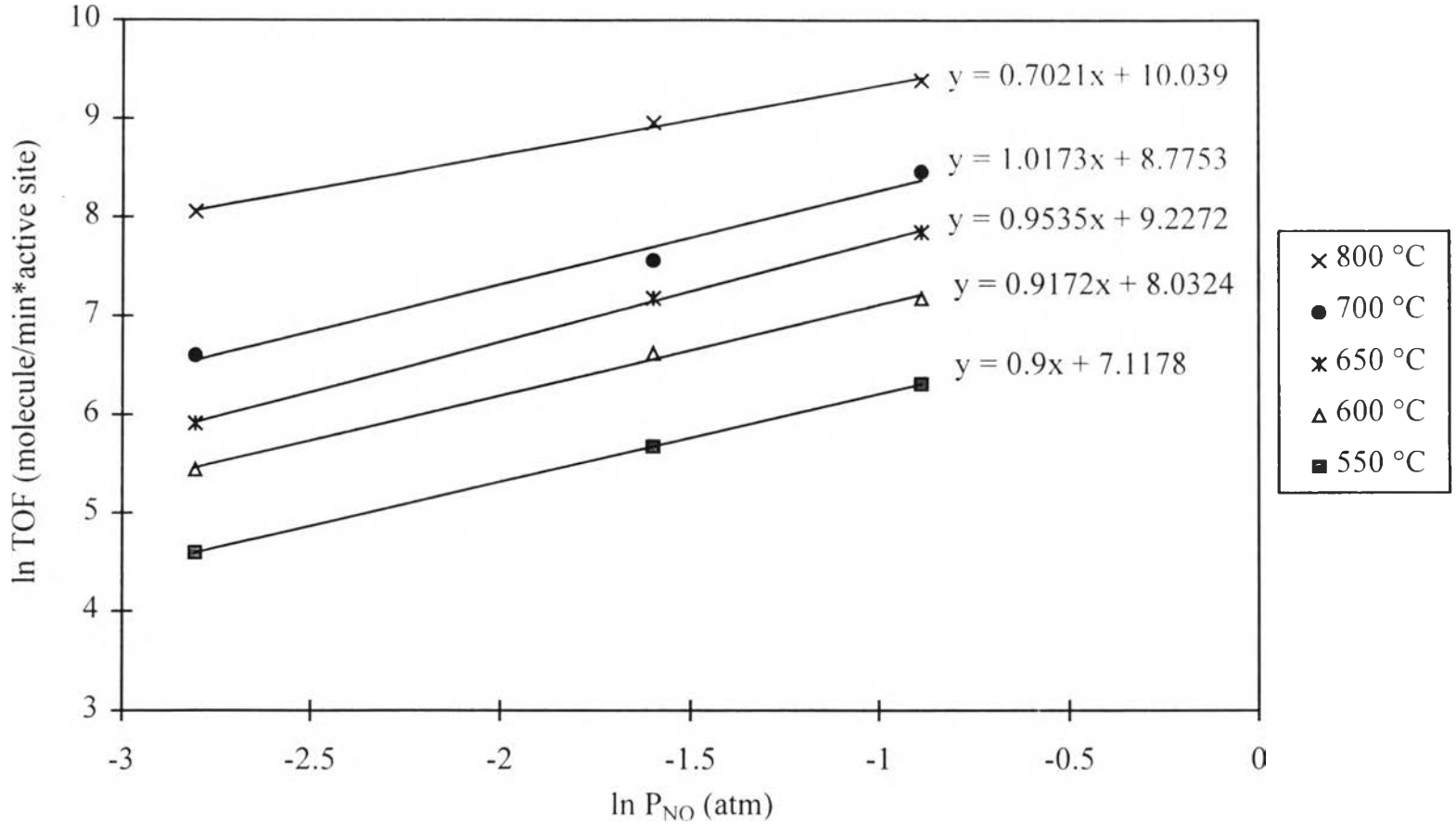

Figure 4.11 Relation between the initial pressure of NO and TOF of NO reduction with SP-1 graphite at temperature between 500-800 °C.

4.3 The Activation Energy

From the rate equation of NO

$$r = kP_{NO}^{a}$$

Substituting the Arrhenius equation, $k = A_0 e^{(-Ea/RT)}$, into the above equation gives

$$r = A_0 P_{NO}^{a} e^{(-Ea/RT)}$$

where r = NO molar reaction (destruction) rate per unit solid surface area per time per unit of NO pressure;

P_{NO} = the initial partial pressure of NO;

a = kinetic order of NO;

A_0 = preexponential factor;

Ea = the activation energy, kJ/mole;

R = a gas constant = 8.314 J/mol·K;

T = absolute temperature, K.

Taking the natural logarithm throughout the obtained equation above yields

$$\ln r = \ln\left(A_0 . P_{NO}^{a}\right) - \frac{Ea}{R}\left(\frac{1}{T}\right)$$

Similarly, if a plot of ln r versus (1/T) gives a straight line whose slope is proportional to the activation energy. The activation energy of the reaction is then determined by varying reaction temperatures under a given condition.

Figures 4.12 and 4.13 show the Arrhenius plots at 6% NO concentration for micro 450 and SP-1 graphite, respectively. It can be observed that, in both cases, there is a "break" in the Arrhenius plot whereby the activation energy of the reaction increases as the temperature rises. The temperatures of the break point occurred at around 600 and 650 °C for micro 450 and SP-1 graphite, respectively. At temperature lower than the temperature "break", the activation energy in both cases was found in the range of 63.8-83.6 kJ/mole which was in agreement with the results of Teng et al., (1992). While above the temperature break, the activation energies were approximately 109.2 kJ/mole for micro 450 graphite and 122.4 kJ/mole for of SP-1 graphite.

The Arrhenius plots of the NO reduction by micro 450 and SP-1 graphites at 20% NO concentration in the temperature range of 500-800 °C are illustrated in Figures 4.14 and 4.15, respectively. Both graphs show no break in the Arrhenius plots. The activation energy for micro 450 was 87.8 kJ/mole and was 93.4 kJ/mole for SP-1.

Figures 4.16 and 4.17 show Arrhenius plots at 40% NO concentration of micro 450 and SP-1 graphites in the same range of temperatures. Neither break in the Arrhenius plots of both graphites are found. The activation energies were 70.9 and 83.2 kJ/mole for micro 450 and SP-1, respectively. The activation energies obtained in this work are listed in Table 4.1.

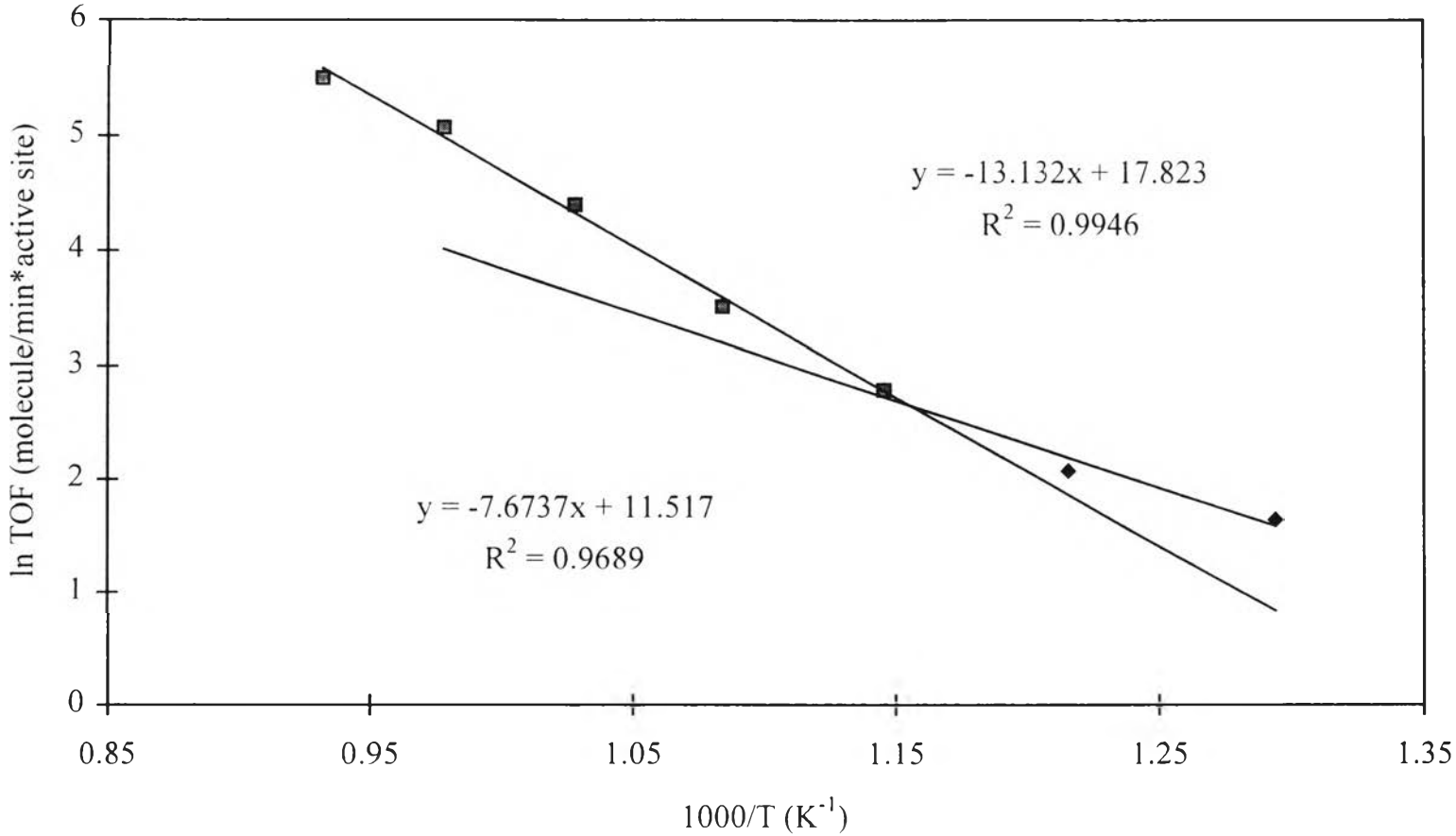

Figure 4.12 Arrhenius plot of micro 450 graphite at 6% NO concentration.

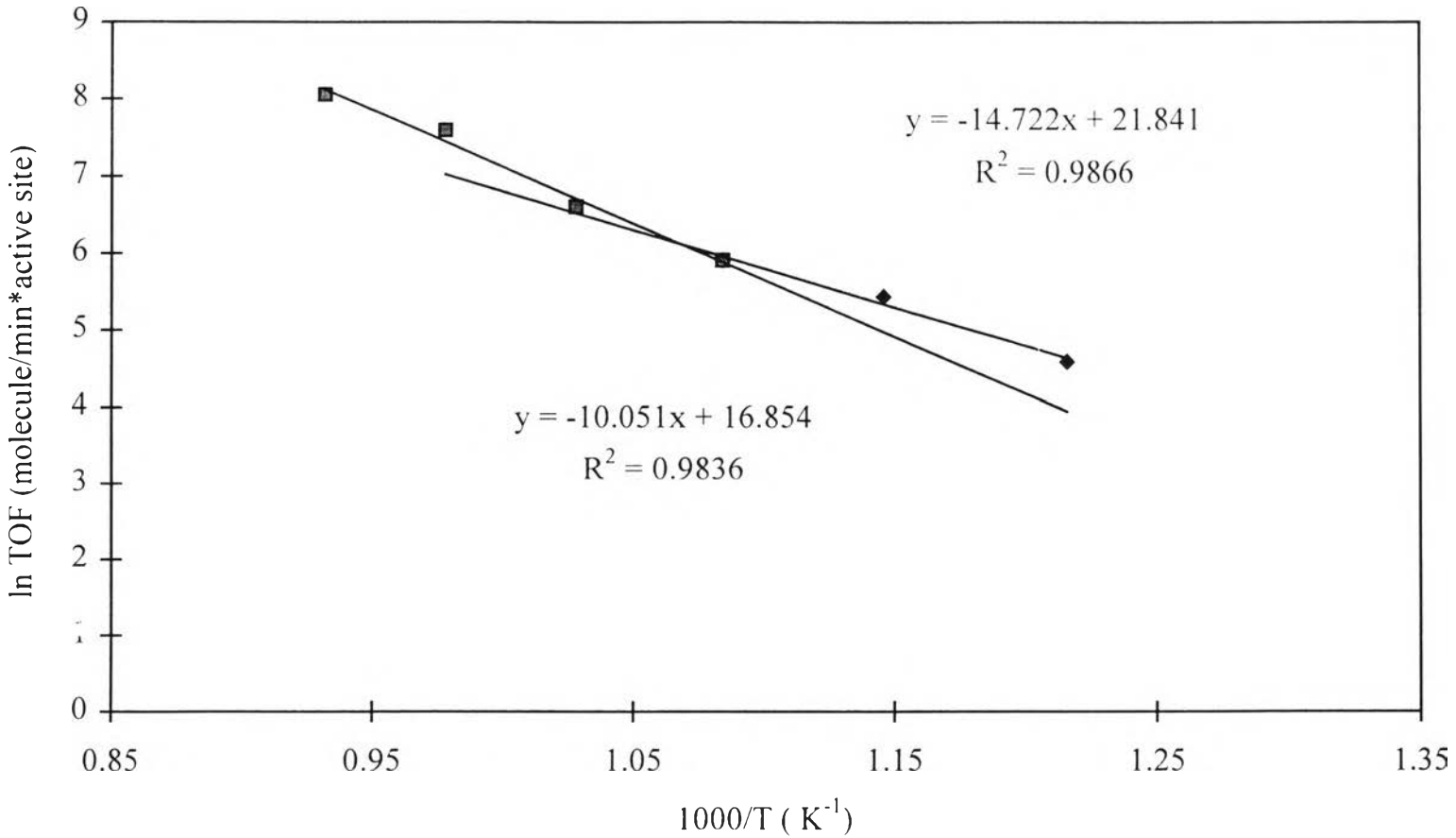

Figure 4.13 Arrhenius plot of SP-1 graphite at 6% NO concentration.

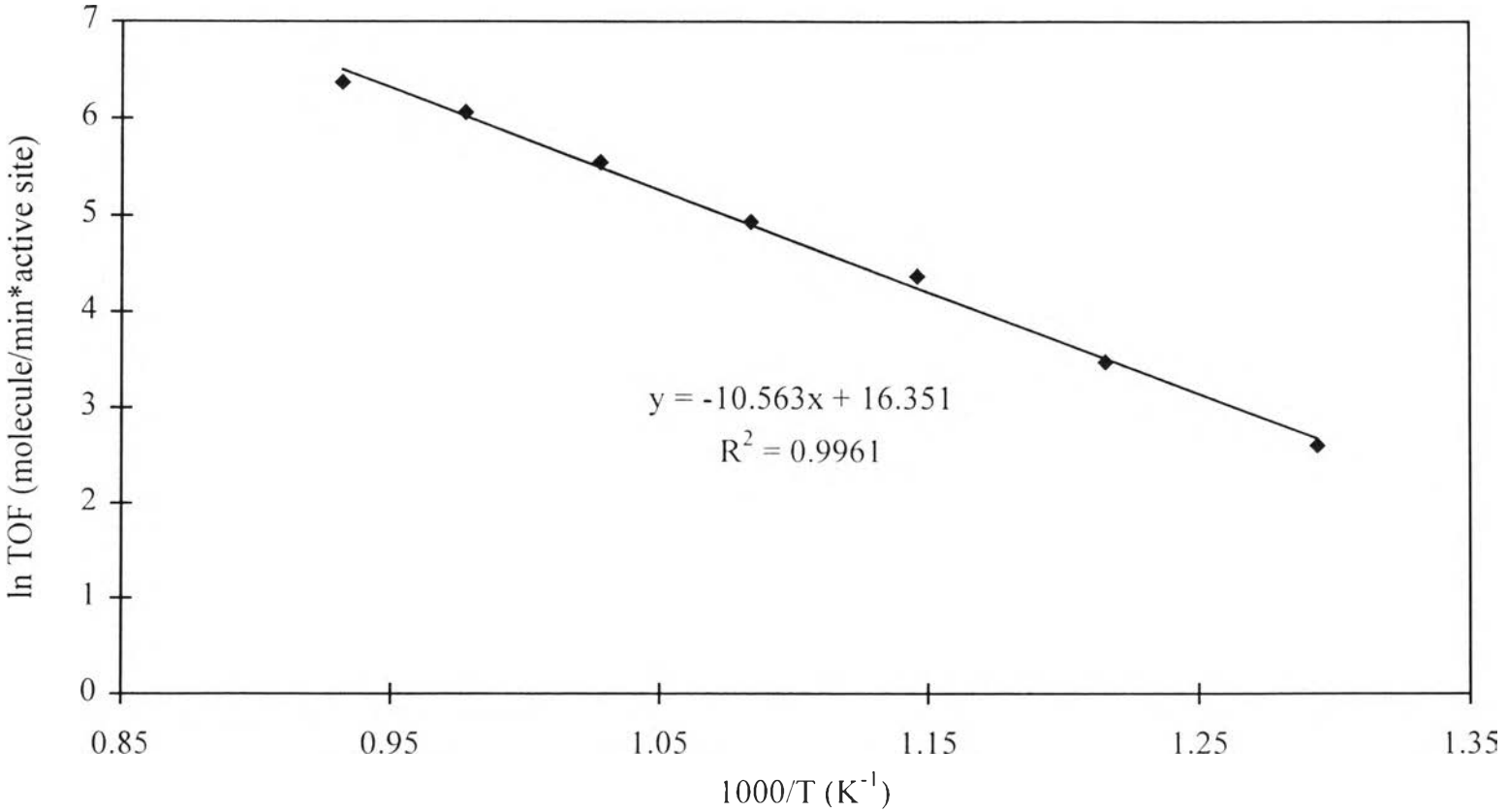

Figure 4.14 Arrhenius plot of micro 450 graphite at 20% NO concentration.

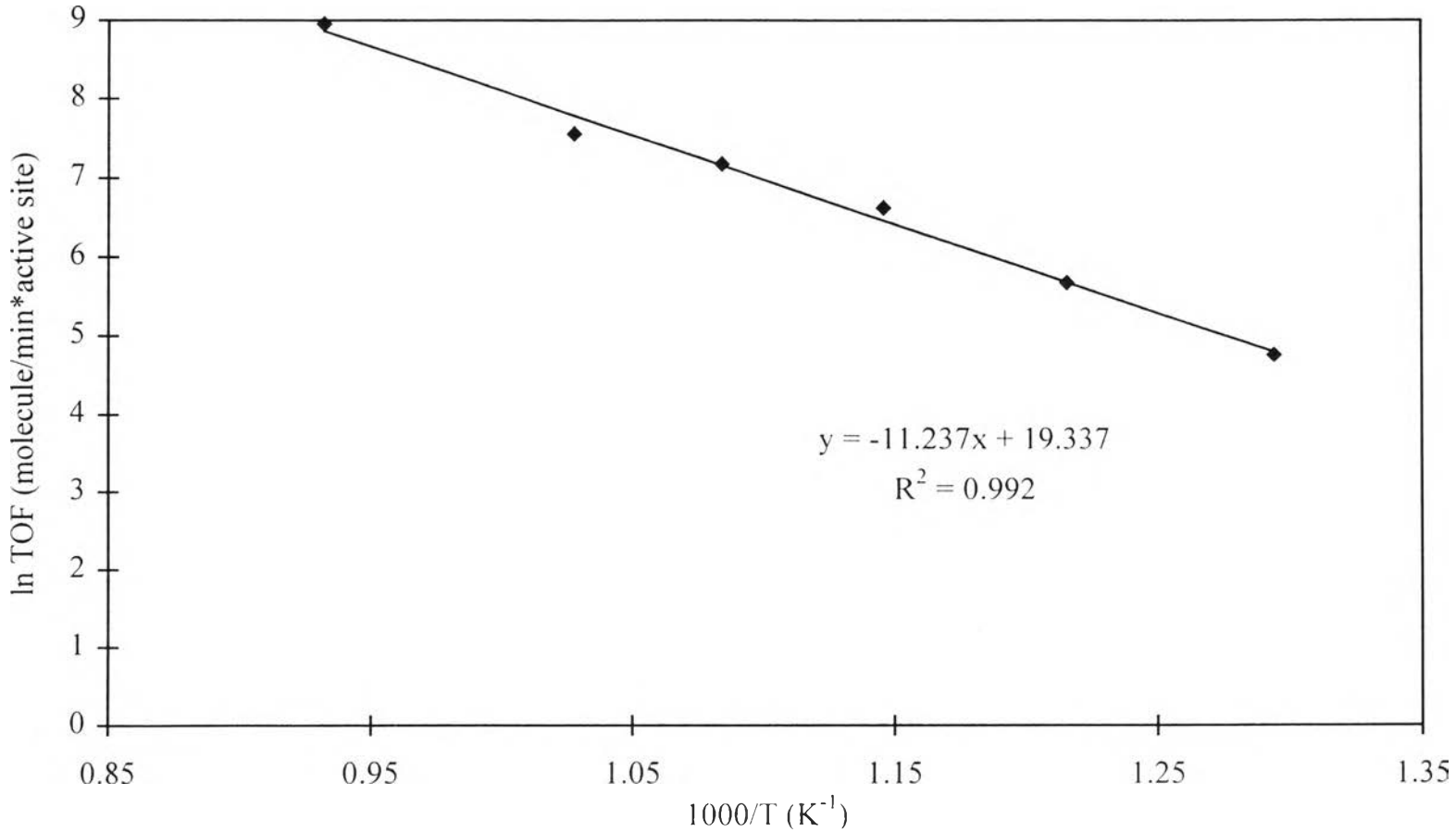

Figure 4.15 Arrhenius plot of SP-1 graphite at 20% NO concentration.

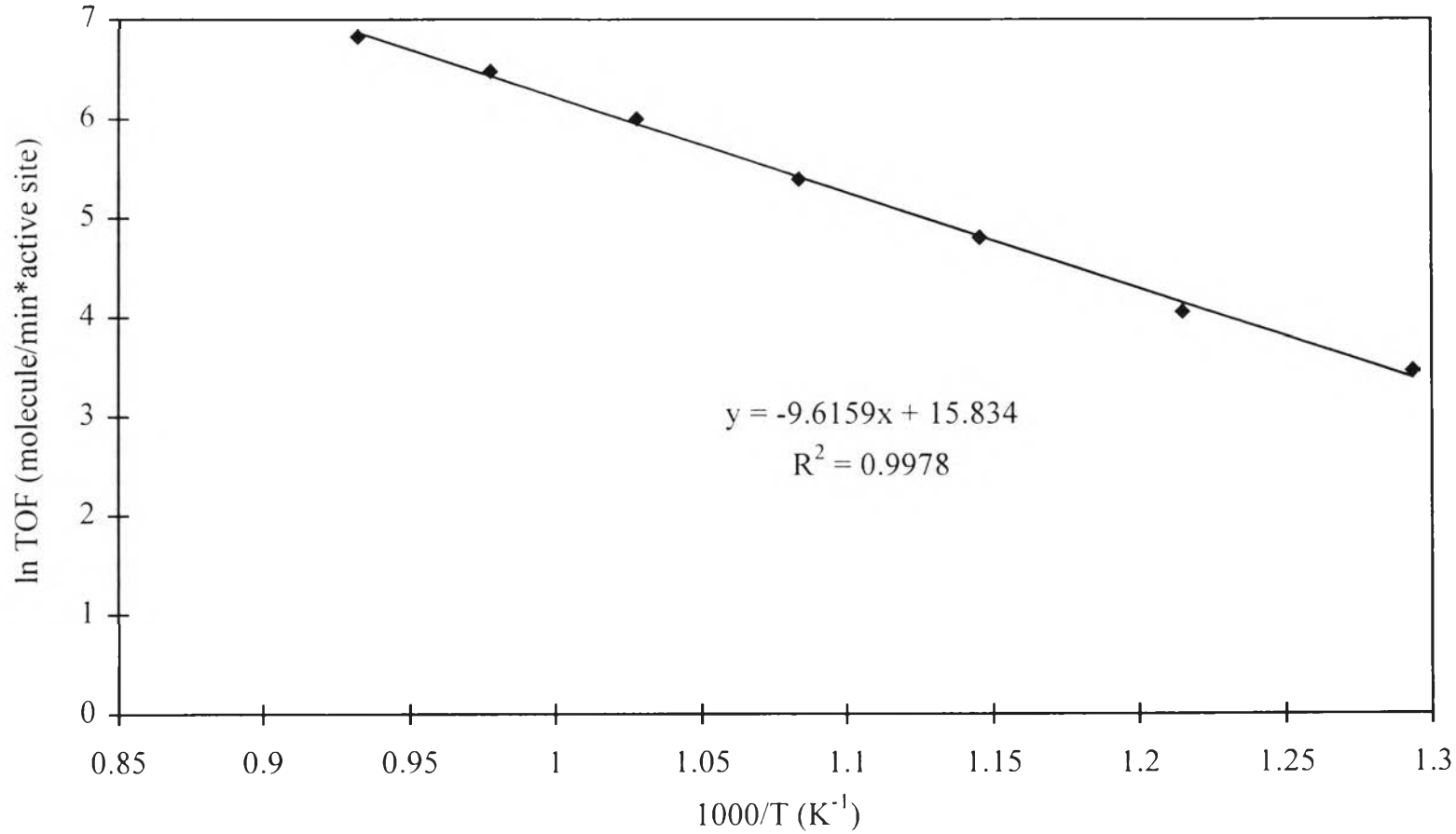

Figure 4.16 Arrhenius plot of micro 450 graphite at 40% NO concentration.

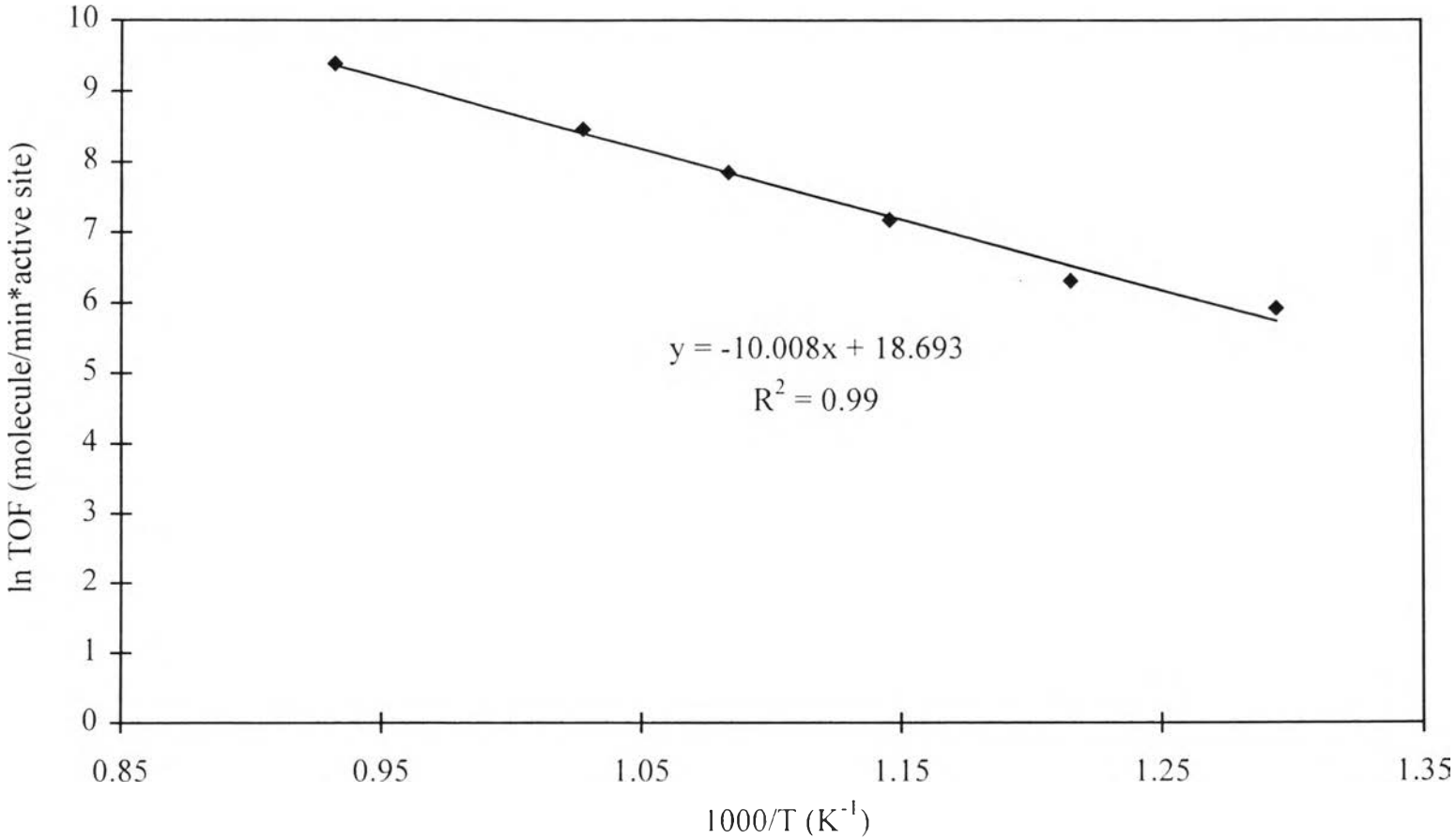

Figure 4.17 Arrhenius plot of SP-1 graphite at 40% NO concentration.

Table 4.1 The activation energy for the NO-graphite reaction in the temperature range of 500-800 °C

graphite	%NO concentration	Ea, kJ/mole	
		low temp.	high temp.
micro 450	6	63.8	109.2
	20	-	87.8
	40	-	79.9
SP-1	6	83.6	122.4
	20	-	93.4
	40	-	83.2

For the dependency of activation energy on the reaction temperature, there were significant changes in activation energy at around 600 °C in case of micro 450 and 650 °C in case of SP-1 at the 6% NO concentration. However, at 20% and 40% NO concentrations, the temperature break cannot be observed.

The reason for the significant change in the activation energy is yet not clear. Furusawa et al. (1980) suggested that the increase in the activation energy might be attributed to a change in the reaction mechanism. They found that the oxygen-carbon complex decreased as the temperature was increased, with none being formed in the region of temperatures where the activation energy rises. The mechanism proposed for reaction between carbonaceous materials and NO:

$$C + NO \longrightarrow \tfrac{1}{2} N_2 + CO \qquad (a)$$

$$C + 2NO \longrightarrow N_2 + CO_2 \qquad (b)$$

$$C + CO_2 \longrightarrow 2CO \qquad (c)$$

At temperature below that at which there was a change in the activation energy, the reaction represented by Equation (a) was the main reaction occurring, while at above that temperature, CO began to form according to either Equation (a) or Equation (c); as the temperature was raised further, the amount of CO formed also increased.

Another suggestion given by Teng et al. (1992) is that they believed the change in the activation energy also caused by a change in the reaction mechanism. In the low-temperature regime (arbitrarily < 650 °C), carbon gasification by NO involves slow desorption of relatively stable surface complexes by a process such as:

$$[\text{surface complexes}] \longrightarrow CO,\ CO_2 \text{ or } N_2$$

The NO-carbon reaction in the high-temperature regime is hypothesized to involve a sequence of NO attack on active unoccupied sites followed by fast product release, which is apparent single-step process:

$$C + NO \longrightarrow CO,\ CO_2 \text{ or } N_2$$

These two different mechanism had the different activation energy. Therefore the activation energy increased when reaction took place above approximately 650 °C as a result of different mechanism.

In this study, it should be noted that the temperature break cannot be observed at NO concentrations other than 6%. This may be because of the increase in the number of NO molecules attacking on unoccupied sites. At high concentration of NO, NO molecules can easily attack on active sites. Therefore the process at high concentration may be only the process involved NO attack on active sites followed by fast product release. This process controls the

overall gasification rate at all range of temperature resulting in no break in the Arrhenius plot. However, more studies are experimentally required to explain this phenomenon.

As seen from Table 4.1, at 40% NO concentration both graphites give lower activation energy than at 20% NO concentration. Thus the NO-carbon reaction is more favorable in higher NO concentration. As stated above, at high concentration of NO, NO molecules have more chances to attack on active sites so that the reaction easily occurs.

Figure 4.18 shows the comparison of the rate constants of the NO gasificaiton reaction by micro 450 and SP-1 graphite with other studies. The rate constants of both graphites in this study are quite high compared with that of other studies. Because in this study the rate constant was calculated based on per active surface area instead of total surface area, the rate constant determined was higher than that calculated based on total surface area. From Figure 4.18, the temperature "break" found (600 °C for micro 450 and 650 °C for SP-1) is in the same range as that found in other studies. It should be noted that the temperature "break" was found in experiments with NO partial pressure of 1.0-10.1 kPa.

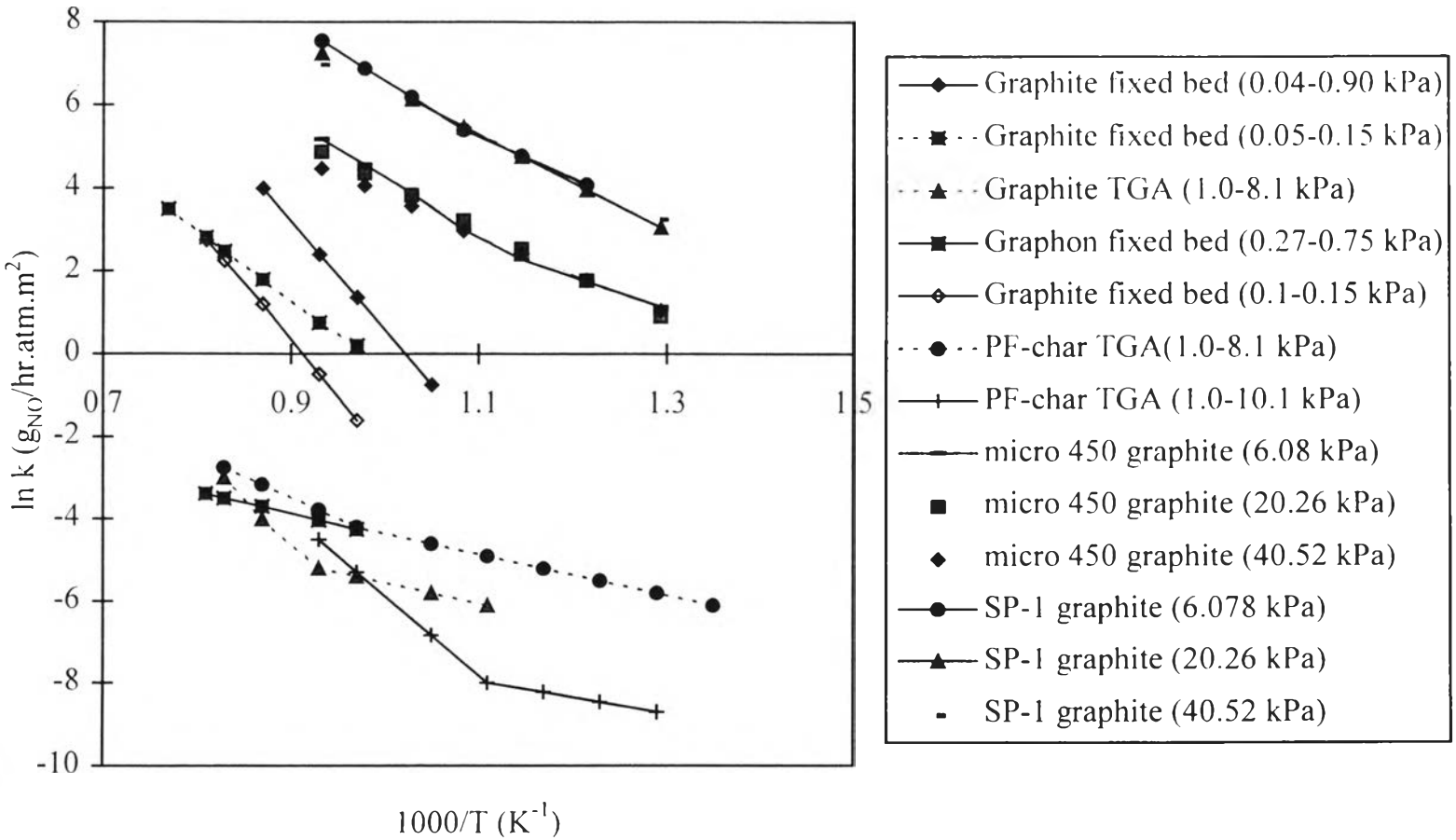

Figure 4.18 Comparison of the rate constant k of the NO-carbon reaction (using micro 450 graphite and SP-1 graphite) with other studies (Aarna and Suuberg, 1997).

Table 4.2 Comparison of the activation energy of the NO-carbon reaction (using micro 450 graphite and SP-1 graphite) with other studies (Aarna and Suuberg, 1997).

Carbon type	Reactor	Temperature Range	NO pressure	Activation energy (kJ/mole)		Reaction	Surface area
		(K)	(kPa)	Low temp.	High temp.	order	(m2/g)
Graphite	Fixed bed	873-1173	0.04-0.90	-	239	1	3.7
Graphite	Fixed bed	973-1223	0.05-0.15	-	162.7	-	13
Graphite	TGA	873-1223	1.0-8.1	65	200	1	17-100
Graphon	Fixed bed	1027-1233	0.27-0.75	-	86.6	1	87
Graphite	Fixed bed	950-1250	0.1-0.15	-	240	-	2
PF-char	TGA	723-1173	1.0-8.1	35	140	-	525-878
PF-char	TGA	773-1073	1.0-10.1	63-88	180	1	2-400
micro 450	TGA	773-1073	6.08	63.8	109.2	1	0.89
micro 450	TGA	773-1073	20.26	-	87.8	1	0.89
micro 450	TGA	773-1073	40.52	-	79.9	1	0.89
sP-1	TGA	773-1073	6.078	83.6	122.4	1	0.054
sP-1	TGA	773-1073	20.26	-	93.4	1	0.054
sP-1	TGA	773-1073	40.52	-	83.2	1	0.054